

FPGA IMPLEMENTATION OF A CONTROL SYSTEM FOR THE LANSCE ACCELERATOR

Sungil Kwon[#], L. Castellano, D. Knapp, M. Prokop, P. Torrez, A. Scheinker, J. Lyles, and D. Rees, Los Alamos National Laboratory, Los Alamos, New Mexico, USA

Abstract

As part of the modernization of the Los Alamos Neutron Science Center (LANSCE), a digital low level RF (LLRF) system was designed. The LLRF control system was implemented in a Field Programmable Gate Array (FPGA) using embedded Experimental Physics and Industrial Control System (EPICS) Input Output Controller (IOC) under the Real-Time Executive for Multiprocessor Systems (RTEMS). Proportional-Integral (PI) feedback controller, static beam feedforward controller, and iterative learning controller are implemented on the FPGA. The closed loop system performance was tested with a 10mA peak current proton beam.

INTRODUCTION

The modernization of the LANSCE 201 MHz RF systems including the LLRF control systems, RF amplifier systems, water-cooling systems and networking is under way[1,2]. Analog low level RF control and electronics have been replaced with FPGA based control systems. The legacy LANSCE LLRF system was an analog PI Feedback control system which provided amplitude and phase error of $< \pm 0.12\%$ and $\pm 0.1^\circ$, respectively. However, it does not support network control or data acquisition of LLRF parameters. The new design of the LLRF system using an FPGA with an embedded softcore processor and network support. Also, the FPGA-based design gives the ability for algorithm and processor modification and upgrade. In this note, an overview of the new LLRF system and the control system performance with a baseline proton beam of LANSCE are addressed.

LLRF SYSTEM OVERVIEW

The LLRF control system is illustrated in Figure 1. It consists of the clock system, analog front end, down converting mixers, FPGA (Stratix III) based control system, the RF power amplifier chain, and a cavity. The clock system generates the FPGA clock and LO signal from the 10MHz reference signal. The mixers are located in the LINAC tunnel, which down-converts the 201.25 MHz cavity and reference RF signal to the 25.15625 MHz intermediate-frequency (IF) signals. These IF signals are filtered by diplexer filters to eliminate the higher order harmonics and fed to 16-bit ADCs (LTC2208) where four times oversampling scheme is used. The ADC output of the reference IF signal is conditioned and is used for IF modulation of the base band I/Q control signals. The I and Q stream outputs of the ADC of the cavity IF signal are

processed to remove the DC offsets and then they are filtered by 150-tap linear-phase low pass FIR filter, yielding baseband cavity field I and Q signals. Meanwhile, the relative phase of the cavity field with respect to the reference is calculated using CORDICs (Coordinate Rotation Digital Computers) from I and Q data of the reference IF signal and I and Q data of the cavity IF signal. The PI control algorithm is applied to the cavity field I and Q signals to obtain the control actions that will be digitally modulated onto control IF signal. A 16-bit DAC (AD9726) transforms the digital control IF signal back to analog IF signal and the analog IF signal is up-converted to the 201.25 MHz control RF. The analog control RF signal is amplified through the RF amplifier chain to the cavity. The LLRF control system parameters are loaded to memory mapped-registers located in the FPGA through the EPICS IOC over the network. For the register reads and writes, and waveform uploads, a CPU softcore, NIOS II processor, is embedded in FPGA and the EPICS IOC on the operating system Real-Time Executive for Multiprocessor Systems (RTEMS).

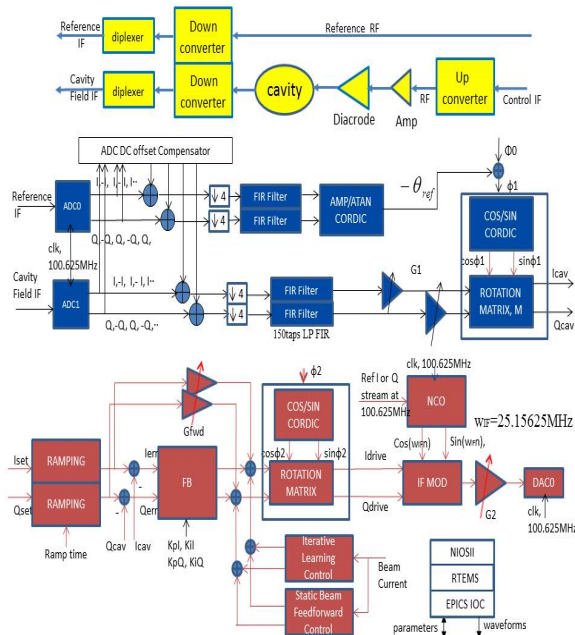


Figure 1: Schematic block diagram of the digital field control module (FCM).

skwon@lanl.gov

FEEDBACK CONTROL PERFORMANCE

Because of the high power requirement of the LANSCE accelerator, two diacodes are installed and their outputs are combined through a hybrid to drive a DTL tank[2]. The performance of the feedback control system is shown figure 2. The PI feedback is applied. The amplitude and phase stabilities are $\pm 0.05\%$ and $\pm 0.05^\circ$, respectively. Note that with higher PI gains, better performance is obtained. However, because there is a loop delay of a few μsec , in order to choose the gains it is necessary to consider the output performance and robustness, input usage and noise sensitivity. In order to confirm the performance of the feedback control, the amplitude and phase are measured with external monitors based on ADL5511 RF amplitude detector and AD8302 Phase Detector. The obtained signals are shown in figure 2 and the amplitude and phase stabilities on the flattop are $\pm 0.04\%$ and $\pm 0.02^\circ$, respectively.

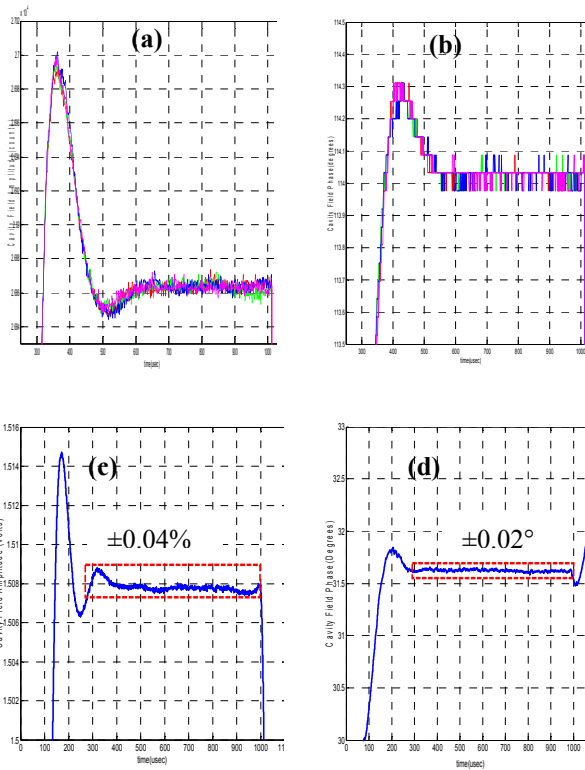


Figure 2: Amplitude and Phase Stabilities of the Feedback System. (a) FCM measured amplitude, (b) FCM measured phase, (c) ADL5511 measured amplitude, (d) AD8302 phase detector measured phase.

BEAM LOADING COMPENSATION BY FEEDFORWARD CONTROLS

Two types of beam loading compensation feedforward controllers are implemented. The first beam feedforward controller is the static beam feedforward controller (SBFFC), where the detected beam current is read-back to the LLRF system and a proper amplification and rotation of the detected beam current generates the feedforward I

and Q control signals. Figure 3 shows SBFFC performance when 10mA production beam having 20usec ramp is operating at 1 Hz rate on LANSCE DTL Tank 2. It is observed that the stabilities on the flattop are $\pm 0.20\%$ and $\pm 0.07^\circ$, respectively. It is noted that around the middle of the beam ramp (10usec), the beam loading effect on the amplitude is not suppressed well (0.58%) though it is improved a lot compared with the case when only feedback controller is applied (Figure 4). This may be improved by a new scheme where the SBFFC enable time is adjusted optimally.

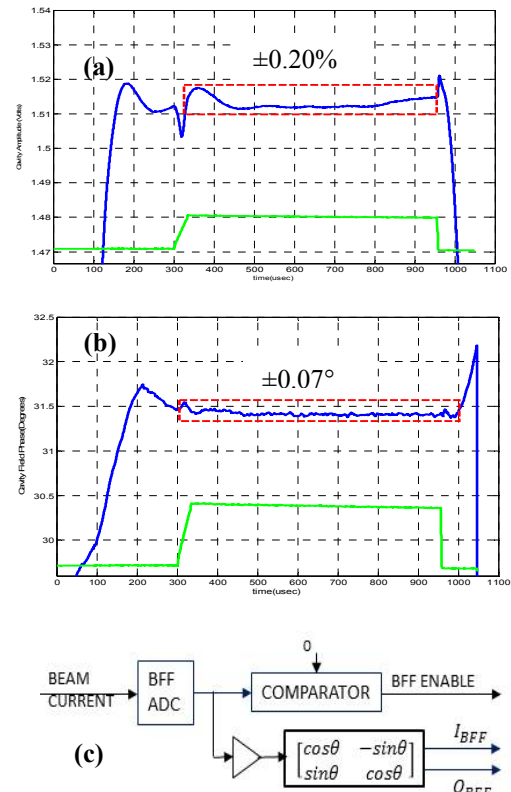


Figure 3: Amplitude and Phase Stabilities of the Static Beam Feedforward Control. (a) ADL5511 RF amplitude detector, and (b) AD8302 Phase Detector. (c) Schematic of SBFFC. Green: Beam Current, 10mA.

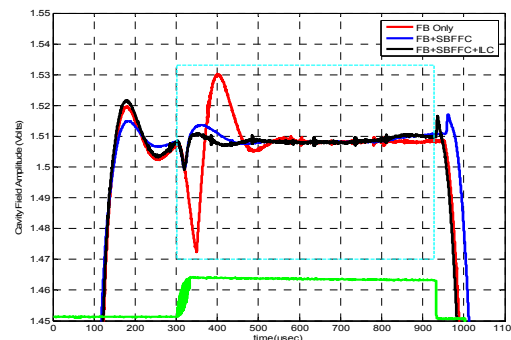


Figure 4: Amplitude stability Comparison. Feedback Only System has 2.3% transient stability. Green: Beam Current, 10mA.

A further improvement is possible by an additional feedforward controller. The second type of the feedforward controller is the iterative learning controller (ILC). The implemented ILC is the current cycle feedforward (CCF) [3]. That is, the controller output updating rule is

$$u_{k+1} = Q(z)u_k + L(z)e_k + u_{FB} + u_{SBFFC}$$

where u_{FB} is the feedback controller and it is given by $u_{FB} = C(z)e_{k+1}$. The reason for this update rule is that the feedforward control is supplementary and the feedback controller is not replaced with ILC and the stability of the closed loop system, which is primarily determined by the PI feedback controller, is preserved. It is noted that the steady state error of the system is affected by the Q filter and L filter. In the implementation of ILC, the Q filter is a first order low pass IIR filter and its gain, q , is adjustable by the user input through EPICS IOC.

$$Q(z) = q \frac{(1-a)}{z-a}, 0 < a < 1$$

The pole, a , of the Q filter is determined so that Q filter does not deteriorate the closed loop system stability. L filter does not filter out the interesting frequency components of the error signal and should not degrade the closed loop system stability. Because of the trade-off of stability and performance, the L filter, high frequency components of the error if there exist may not be suppressed.

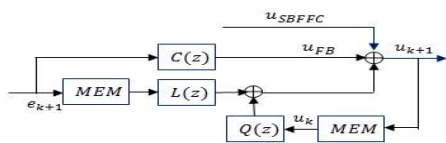
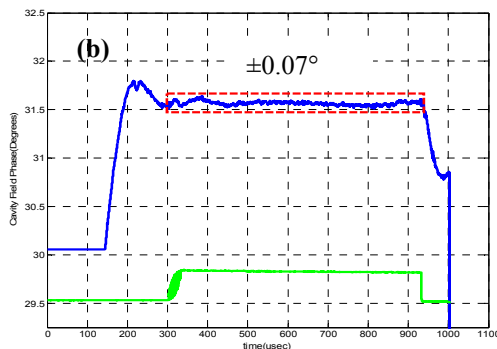
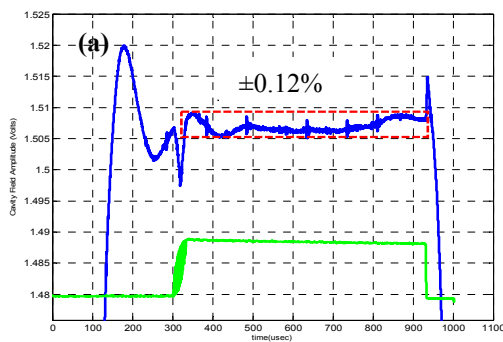


Figure 5: Amplitude and Phase Stabilities of the Adaptive Feedforward Control. (a) ADL5511 RF amplitude detector, and (b) AD8302 Phase Detector. (c) Schematic of ILC. (Green: Beam Current, 10mA).

Figure 5 shows the cavity field amplitude and phase when ILC is applied together with the PI feedback controller and SBFFC after the error converges to the steady state. It is known that there is a stabilizing equivalent feedback controller of the CCF and its equivalent controller characteristics is determined by the Q filter and the L filter [3]. In addition, when the error converges, the closed loop system with CCF type ILC converges to the equivalent feedback controller and no more performance improvement is obtained. Due to the same reason as addressed in the static beam feedforward control, the initial beam loading transient is not compensated well, but at flattop, the amplitude and phase stabilities are $\pm 0.12\%$ and $\pm 0.07^\circ$, respectively.

PHASE SCAN

In order to accelerate a beam, it is necessary to find the optimal acceleration field point. This is performed by scanning the phase under the constant amplitude. During the phase scan, the cavity field amplitude variation should be as small as possible. Figure 6 shows the amplitude variation versus the phase set points. Small amplitude variation is observed though it is within $\pm 0.11\%$. This is caused by mixer nonlinearity, channel crosstalk in the downconverter, other nonlinear distortion in the RF receiving path.

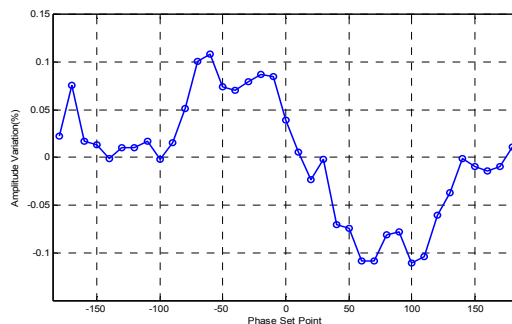


Figure 6: Amplitude Stability at 360 degree phase scan.

CONCLUSION

The digital LLRF system has been installed at LANSCE DTL tank 2. The compensation performance of feedforward controls with the LANSCE 10mA proton beam yields very promising results in terms of amplitude and phase stabilities.

REFERENCES

- [1] D. Rees *et al.*, "LANSCE RF Systems Improvements for Current and Future Programs, in *Proc. IPAC'11*, San Sebastian, Spain, Sep. 2011, paper MOPC068, p. 238.
- [2] J. Lyles *et al.*, "Installation and Operation of Replacement 201 MHz High Power RF System at LANSCE," in *Proc. IPAC'15*, Richmond, Virginia, USA, Jun. 2015, paper WEPWI002, p. 3485.
- [3] M. Verwoerd *et al.*, "On admissible pairs and equivalent feedback-Youla parameterization in iterative learning control," *Automatica*, vol.42, pp. 2079-2089, 2006.